Kovove Mater. 61 2023 223–231
DOI: 10.31577/km.2023.4.223

Effect of plasma spraying parameters on microstructure and thickness and porosity of WC-CrC-Ni coatings deposited on titanium

Krzysztof Szymkiewicz[1], Marek Góral[2], Tadeusz Kubaszek[2], Kamil Gancarczyk[2]

[1] *Cracow University of Technology, Department of Applied Mechanics and Biomechanics,*
24 Warszawska st., 31-155 Kraków, Poland
[2] *Research and Development Laboratory for Aerospace Materials, Rzeszów University of Technology,*
12 Powstańców Warszawy st., 35-959 Rzeszów, Poland

Received 18 November 2022, received in revised form 20 January 2023, accepted 4 April 2023

Abstract

Thermal spraying allows forming of protective coatings with high wear and corrosion resistance, which are successfully applied in the aviation industry on an aircraft engine. In the presented paper, the WC-CrC-Ni carbide coatings on titanium substrate with the use of an Atmospheric Plasma Spraying (APS) process were formed. The aim of this work was to determine optimal APS plasma spraying parameters, which will allow producing the relatively thick coating with as low as possible porosity. The microstructure of obtained carbide coatings was observed with the help of the optical microscope (OM) and scanning electron microscope (SEM). Moreover, the phase composition of produced coatings using X-ray diffraction (XRD) was determined. The obtained results of investigations revealed that the appropriate selection of process parameters (powder feed rate, power current, and plasma gases H_2/Ar flow ratio) allows producing the relatively thick coatings, which are characterized by low porosity.

Key words: WC-CrC-Ni, carbide coating, plasma spraying, microstructure

1. Introduction

Titanium and its alloys are characterized by high specific strength and corrosion resistance; therefore, they are successfully applied in various industries, including aerospace. Nevertheless, their relatively low hardness causes them to suffer from fast wear. It seems to be that the appropriate way to overcome this drawback could be the formation of a metaloceramic protective coating with significantly improved wear and erosion resistance of treated parts [1]. The thermal spraying (TS) process is a well-known method for the production of hard metaloceramic coatings to protect base material against wear and erosion [2, 3]. The high-velocity oxygen fuel (HVOF) process is mainly used for thermal spraying of WC and CrC-containing powders in Ni/Cr/Co matrix [4]. The main advantage of the HVOF process is the very low porosity of the coating according to the higher velocity of powder particles and lower temperature of the plume [5]. The metaloceramic coatings contain both types of carbides (WC and CrC) and may be used in different applications like coal power plants [6]. The CrC-NiCr coating is a promising alternative to hard chrome plating [7] for valves and pistons. The WC and CrC-containing layers might be also manufactured by the detonation-spray method [8]. Picas et al. [9] proposed the production of duplex coating by HVOF-spraying of Cr_3C_2-NiCr coating and CrN deposition using the PVD method. The dry-sliding wear properties of WC, as well as WC-(WC,Cr)2C3 containing HVOF-sprayed coatings up to 750 °C, were investigated by Bolelli et al. [10]. The high influence of temperature on the wear resistance of the layer was observed. The mechanism of indentation fracture toughness was investigated by Š. Houdková and M. Kašparová [11]. Rahbar-Kelisham improved the wear resistance of flame-sprayed WC-12Co coating using the friction stir welding method [12]. Kumar et al. [13] proved that using of high-velocity air fuel process

---

*Corresponding author: e-mail address: krzysztof.szymkiewicz@pk.edu.pl

(HVAF) increases the erosion resistance of WC-CoCr coating in comparison with the conventional HVOF process. The increasing of hard particles of CrC content in CrC-NiCrFeSiBCoC also increased the wear resistance of HVOF coating [14]. Corrosion properties of HVOF-sprayed WC/CrNi and WC/CrC/CoCr were investigated by V. A. D. Souza and A. Neville [15]. The presence of chromium in carbide metaloceramic coatings increases their corrosion resistance [16].

The metaloceramic coatings might be also produced by other TS methods, such as Atmospheric Plasma Spraying (APS), as an alternative to HVOF [17]. Actually, different types of plasma-sprayed wear-resistant coatings were investigated, including NiCrB-SiCFe [18], NiCrSiB/Al_2O_3 [19] NiCrBSi, NiCrBSi/WC-Ni, NiAl [20]. The wear properties of APS-sprayed WC-Co coatings as an alternative to hard chromium were investigated by Balamurugan et al. [21]. The plasma transfer arc (PTA) might be also used for the production of WC-Ni coating [22]. Wear resistance of plasma sprayed Cr_3C_2-NiCr coating might be improved by the addition of B_4C and Cr_2O_3 [23]. There are not many references for metal-ceramic materials containing both CrC and WC carbides. Huang performed comparative studies of WC-CrC-Ni powders produced by different manufacturers [24]. The corrosion resistance of this type of coating was investigated by Murariu et al. [25]. Richert et al. analysed the influence of LPPS plasma spraying parameters on the microstructure of WC-CrC-Ni coating [26]. The mechanical properties of HVOF-sprayed coatings were investigated by Jonda and Latka [27]. In our previous research, we analysed the microstructure and wear properties of plasma-sprayed WC/Co [28] and WC-Cr-Ni [29] powders. In the present article, we analysed the relationship between plasma spray process parameters on microstructure and porosity of WC-CrC-NiCr coatings formed on titanium Grade 2 substrate material.

Table 1. Chemical composition of Ti Grade 2 (wt.%)

Fe	C	N	O	H	Ti
0.3	0.08	0.03	0.25	0.015	Bal.

2. Materials and methods

Commercial pure titanium Grade 2 was used as the substrate material. The as-supplied material, except titanium, was also composed of a small amount of iron, carbon, oxygen, and hydrogen (Table 1).

Before the plasma spraying process, the thin plates (with 2 mm of thickness) were subjected to sandblasting treatment, aimed to obtain uniform surface roughness. Next, the surfaces of the samples were cleaned with isopropanol. The feedstock material was powder SJA 175 WC-CrC-Ni supplied by Thermico (Germany). The composition of the powder was as follows (wt.%): WC-73 %, CrC-20 %, and Ni-7 %. The average grain size of the powder was 17 μm ± 3 μm. The detailed characteristic of powder particles (i.e., particle size distribution) was investigated and described in our previous paper [29].

The thermal spraying process was performed by the APS method with the use of a single-electrode A60 plasma torch (Thermico, Germany). The spray distance was 100 mm. The carrier gas flow rate and process time were 6 NLPM (normal litre per minute), and 180 s, respectively. In the experimental plan, different variables were changed, including powder feed rate, power current, and Ar/H_2 flow ratio (Table 2).

The cross-sections of obtained coatings were embedded in the conductive resin. Next, the surfaces of the samples were ground using sandpapers with a grit size of 220 to 5000. After that, the metallographic samples were mechanically polished using colloidal silica suspension (0.04 μm). The microstructure observations of specimens prepared in this way were

Table 2. Parameters of air plasma spraying process

No.	Plasma gases flow rate (NLPM)		Power	Voltage	Torch current	Powder feed rate	Carrier gas flow (Ar)	Process time
	Ar	H_2	(kW)	(V)	(A)	($g\,min^{-1}$)	(NLPM)	(s)
1	68	5	27.4	61	450	20	6	~ 180
2	68	5	27.5	61.2	450	10	6	~ 180
3	68	5	27.7	61.8	450	5	6	~ 180
4	68	5	31.6	57.4	550	5	6	~ 180
5	68	5	21.6	62.1	350	5	6	~ 180
6	63	10	28.6	63.6	350	5	6	~ 180
7	73	0	15.5	34.6	350	5	6	~ 180

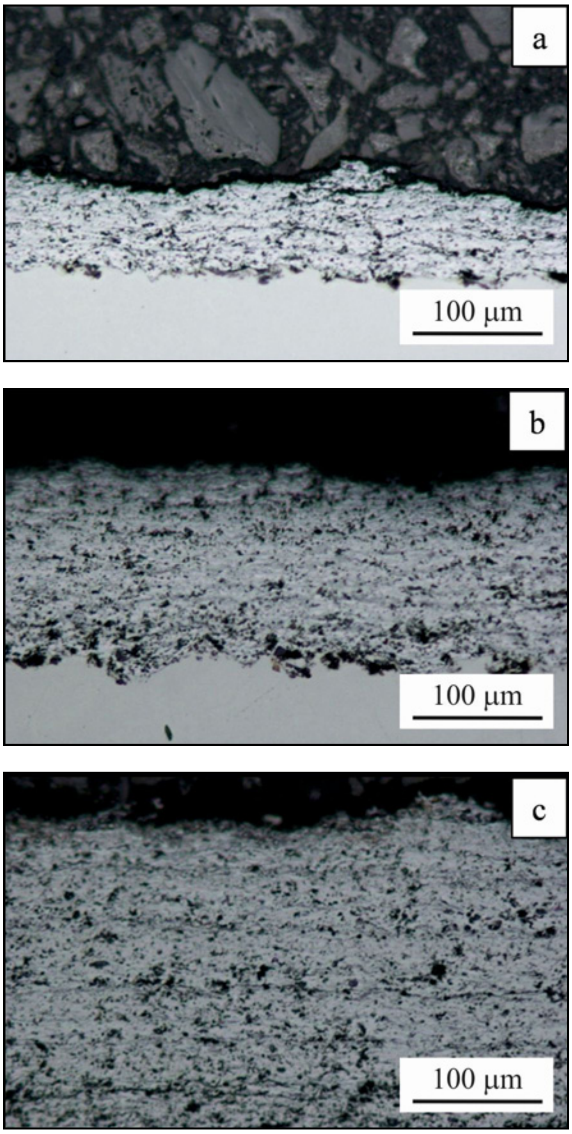

Fig. 1. OM images of cross-section of WC-CrC-Ni coatings plasma sprayed on titanium Grade 2 substrate at variable powder feed rate: (a) $5\,\mathrm{g\,min^{-1}}$, (b) $10\,\mathrm{g\,min^{-1}}$, and (c) $20\,\mathrm{g\,min^{-1}}$.

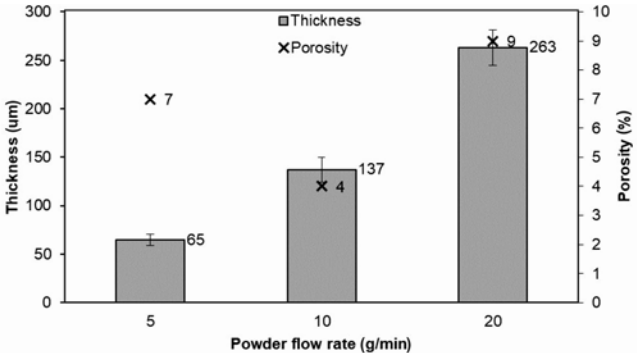

Fig. 2. Thickness and porosity of WC-CrC-Ni coating in dependence on powder flow rate.

carried out by means of a Nikon Epiphot 300 optical microscope equipped with a digital camera. The local microstructure of WC-CrC-Ni carbide coatings was observed by Philips XL 30 scanning electron microscope (SEM). The observations were performed with the use of backscattering electrons (BSE) mode. The measurements of porosity and thickness of coatings were performed with the use of ImageJ and Gatan GMS 3 software, respectively.

The phase analysis of plasma sprayed coatings and substrate material was determined using an XTRa ARL X-ray diffractometer. The investigation was performed with the use of Cu Kα radiation and wavelength λ of 0.154 nm. The experiments were performed using monochromatic radiation with a range of 2θ angle from 20° to 90°. The scan range was 20°–100°, the scanning step was 0.02°, and the counting time was 3 s.

3. Results

3.1. Influence of powder feed rate

The microstructures of the cross-section of plasma sprayed coatings produced at different powder feed rates are presented in Fig. 1. It was observed that an increase in powder flow rate led to the growth of coating thickness. The thinnest layer was achieved for the lowest value of powder feed rate, while for $20\ \mathrm{g\,min^{-1}}$, it was even 4 times thicker. All studied coatings were characterized by the presence of pores, which are observed in the form of dark equiaxial areas. Moreover, these layers exhibit numerous longitudinal cracks, which are located between sublayers. The number of observed sublayers corresponded to the number of plasma torches passing over samples during spraying.

The performed investigations indicated that changes in powder feed rate value directly affect the growth of thickness of plasma sprayed coating. The thickness measurements showed that the growth of the coating was almost linear. For the lowest value ($5\,\mathrm{g\,min^{-1}}$), the obtained coating was the thinnest, while the two and four times increase of powder feed rate led to producing even two and four-time thicker WC-CrC-Ni coating, i.e., 137 and 263 µm, respectively. The studies also revealed that plasma sprayed coating produced at $10\,\mathrm{g\,min^{-1}}$ of powder flow rate was characterized by the lowest porosity (4 %). Both rise, as well as decrease of considered/analysed parameters, caused the formation of more porous layers, i.e., 9 and 7 %, respectively (Fig. 2).

The analysis of X-ray spectra registered from substrate materials in the as-supplied form revealed the presence of three strong characteristic peaks located

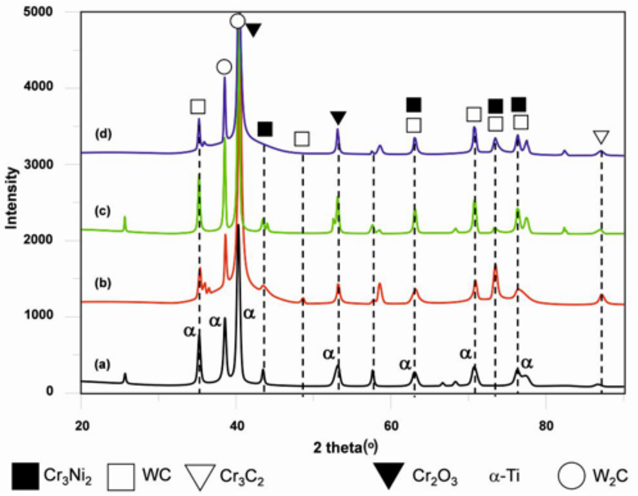

Fig. 3. X-ray diffraction spectra of as-supplied commercial purity titanium Grade 2 (a) and WC-CrC-Ni coatings sprayed at variable powder flow rate: 5 g min^{-1} (b), 10 g min^{-1} (c), 20 g min^{-1} (d).

at 2θ angles (35°, 38°, 41°), which corresponded to the hexagonal form of the α-Ti phase (Fig. 3). Moreover, the low intensity reflex at a higher range of 2θ angle was observed. Their presence can be related to forming of oxide thin layers on the surface of samples. The analysis of X-ray spectra obtained from carbide plasma sprayed coatings with variable powder feed rate indicated that they are composed of two forms of tungsten carbide like WC and W_2C, and Cr_3C_2 chromium carbide. Moreover, the investigations helped to establish that coatings were also formed by Cr_2O_3 chromium oxide, as well as the presence of the Cr_3Ni_2 phase. The analysis of all obtained spectra did not reveal characteristic lines associated with the α-Ti phase, which resulted from the significant thickness of APS coating compared to the depth of interaction of the X-ray beam with the studied material.

3.2. Influence of power current

Microstructure observations of the cross-section of carbide coatings showed that the increase of torch power current from 350 up to 550 A led to obtaining relatively thinner coatings. The coatings obtained at $I = 350$ A were slightly lower than 200 µm, while the further increase of torch current caused the production of twice thinner coatings. The investigations of coatings produced for higher values of power current also revealed the presence of longitudinal cracks, which probably appeared as a result of the solidification process of coatings (Fig. 4). Furthermore, microstructure observations helped to establish that the amount of coating defects increases with increasing torch current.

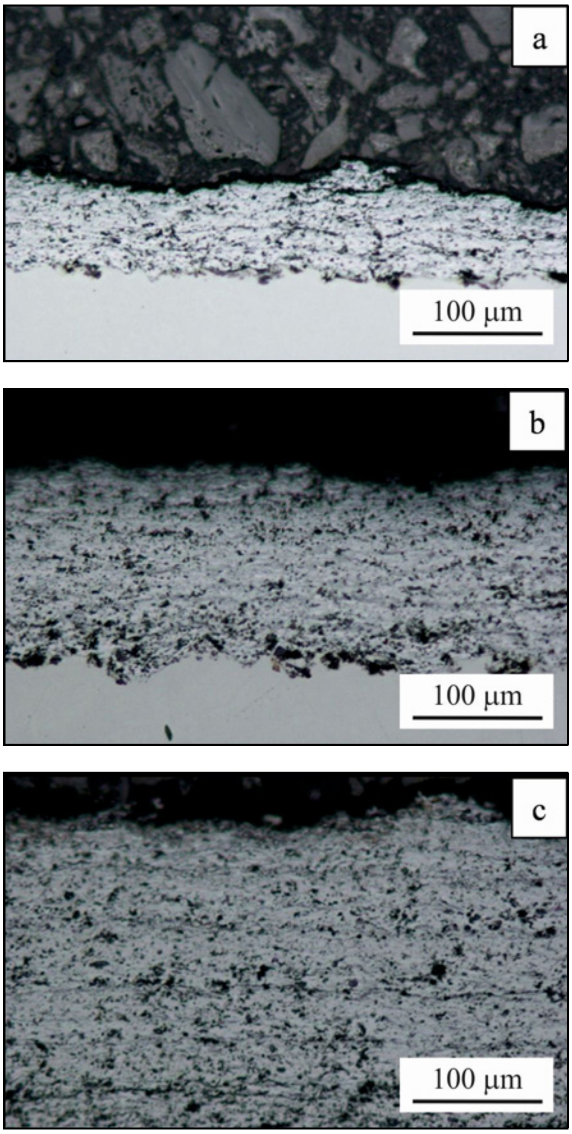

Fig. 4. OM images of cross-section of WC-CrC-Ni coatings obtained at variable torch current: (a) 350 A, (b) 450 A, and (c) 550 A.

Plasma spraying process performed at the lowest power current (350 A) allowed to form the thickest WC-CrC-Ni coating. The further increase of power current led to obtaining significantly thinner coatings. It was mentioned that in the case of a power current of 450 A, a drastic decrease in layer thickness to 65 µm was observed, which can be related to unexpected problems that occurred during the APS process. The porosity measurements of plasma sprayed WC-CrC-Ni coatings showed that it increased with the power current. The coatings obtained at 350 and 450 A were characterized by relatively low porosity in the range of 6–7 %. The coating produced at the highest value of power current exhibited significantly higher porosity (Fig. 5).

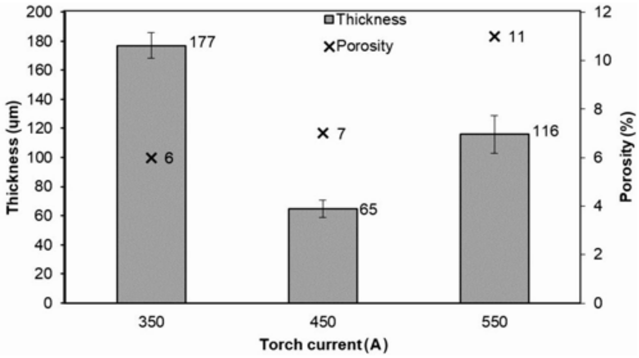

Fig. 5. Thickness and porosity of WC-CrC-Ni coating depending on the torch current.

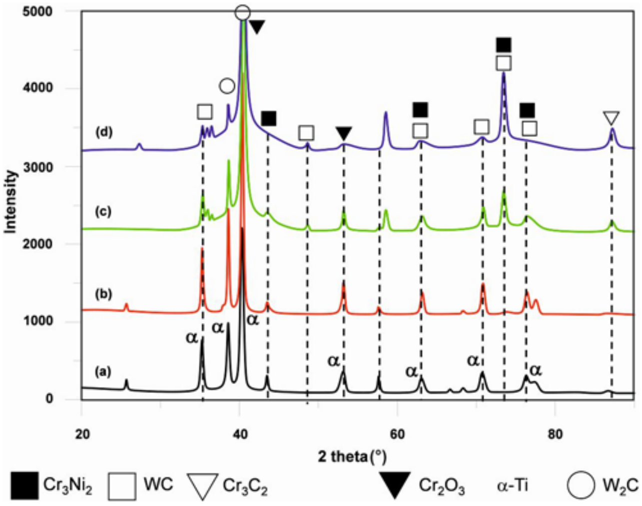

Fig. 6. X-ray diffraction spectra of as-supplied commercial purity titanium Grade 2 (a) and WC-CrC-Ni coatings sprayed at variable torch current: (b) 350 A, (c) 450 A, and (d) 550 A.

The X-ray diffraction patterns were also obtained from the surface of plasma sprayed WC-CrC-Ni coatings produced at variable power current (Fig. 6). The analysis of obtained spectra showed the similar phase composition of coatings, i.e., tungsten carbide (WC and W_2C), chromium carbide Cr_2C_3, chromium oxide Cr_2O_3, as well as Cr_3Ni_2 phases. It was observed that increasing torch current decreases the intensity of characteristic peaks corresponding to the tungsten carbide phase while increasing in the case of the W_2C phase.

3.3. Influence of H_2/Ar flow ratio

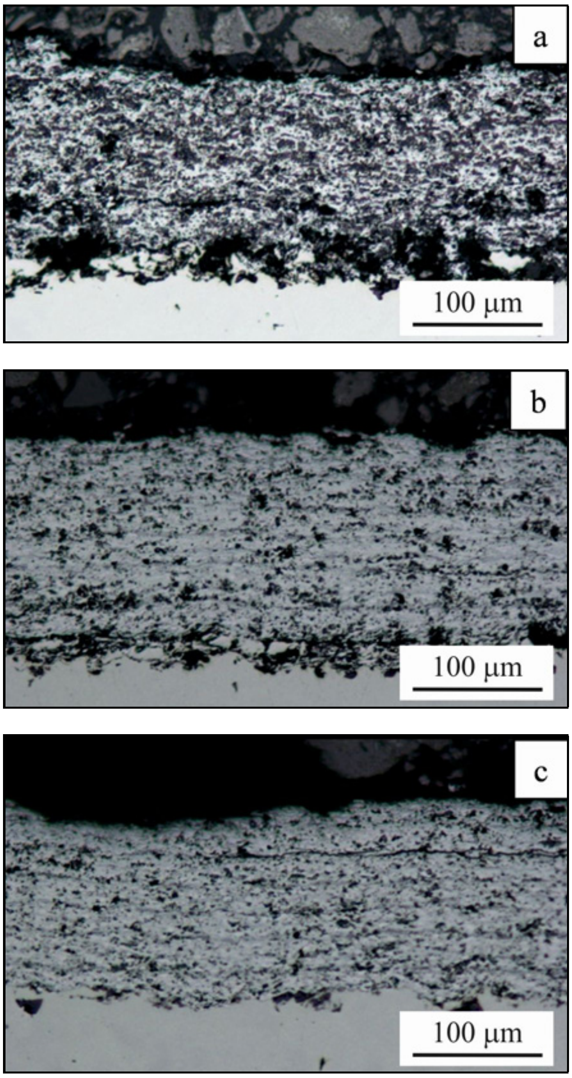

Fig. 7. OM images of cross-section of WC-CrC-Ni coatings produced at variable flow rate of plasma gases H_2/Ar (NLPM): (a) 0/73, (b) 5/68, and (c) 10/63.

Observations of plasma sprayed coatings obtained at variable H_2/Ar flow ratio indicated that the application of only argon gas led to obtaining a layer with higher porosity. Simultaneously, the plasma gases mixture H_2/Ar in the ratio of 5/68 and 10/63 NLPM allowed producing less porous carbide coatings. It should be noted that the application of both gases in the plasma spraying process caused the formation of cracks between individual sublayers (Fig. 7).

The thickness measurements of WC-CrC-Ni sprayed coatings showed that the addition of hydrogen as secondary gas in a mixture of plasma in the ratio H_2/Ar – 5/68 NLPM contributed to producing slightly thicker coatings (177 µm) compared to those formed without using hydrogen (158 µm). It was observed that further increasing of hydrogen amount in the gas mixture led to obtaining a thinner coating. Nevertheless, all produced coatings were characterized by relatively similar thicknesses (approx. 160 µm). The porosity analysis of carbide coatings revealed that using only argon as plasma gas caused the formation of high porosity coating

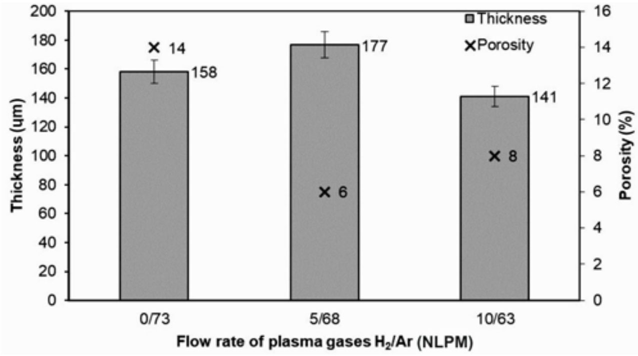

Fig. 8. Thickness and porosity of WC-CrC-Ni coating depending on the flow rate of plasma gases (H_2/Ar).

(14 %). Increase in hydrogen flow rate (H_2/Ar) from 5/68 up to 10/63 NLPM caused a significant lowering of coating porosity, i.e., 6 and 8 %, respectively (Fig. 8).

The X-ray spectra from carbide coatings produced at a variable flow rate of plasma gases H_2/Ar are similar to those obtained for other above-presented results (Fig. 6). The phase analysis also confirmed the presence of carbides (WC, W_2C, and Cr_3C_2), oxide (Cr_2O_3), and Cr_3Ni_2 phases (Fig. 9).

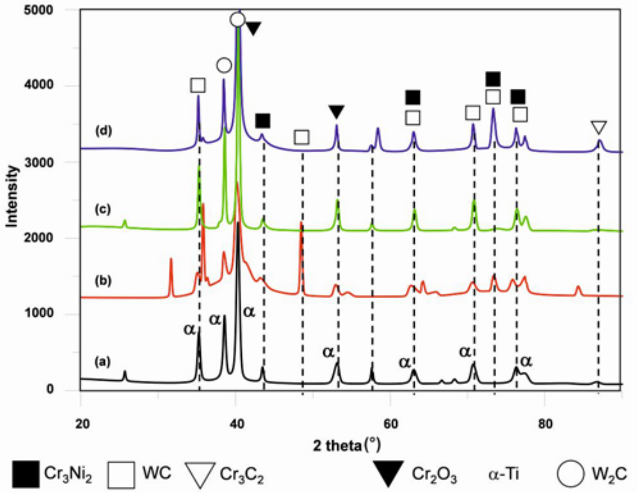

Fig. 9. X-ray diffraction spectra of as-supplied commercial purity titanium Grade 2 (a) and WC-CrC-Ni coatings sprayed at variable flow rate of plasma gases (NLPM) H_2/Ar: (b) 0/73, (c) 5/68, and (d) 10/63.

3.4. SEM local microstructure observations of WC-CrC-Ni coatings

The SEM microstructure observations of the cross-section of the WC-CrC-Ni coatings revealed that such plasma-sprayed coatings have a laminar struc-

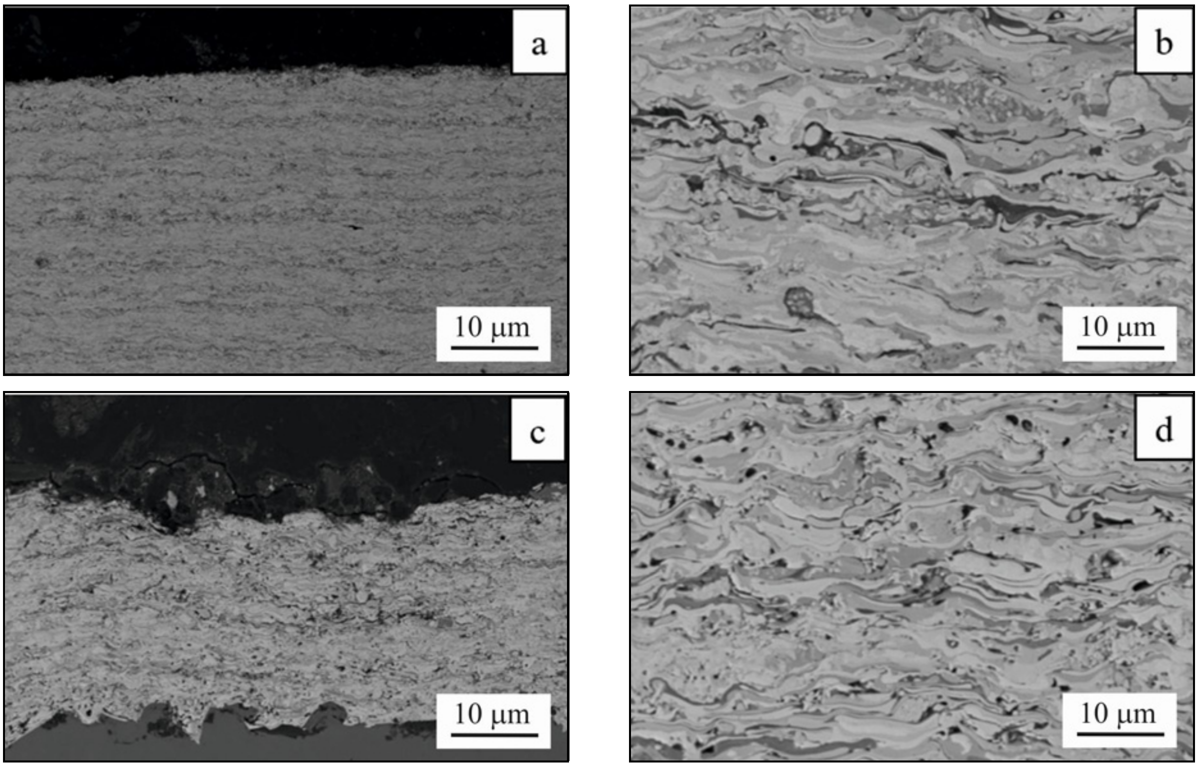

Fig. 10. SEM/BSE images of WC-CrC-Ni coatings sprayed at variable powder feed rate: (a), (b) 20 g min^{-1} and (c), (d) 10 g min^{-1}.

ture (Figs. 10a,c). The coatings are composed of sublayers, the number of which corresponds to the individual torch runs. The dark interface between them was observed. It could have been the result of the formation of oxide compounds during coating crystallization. Moreover, the single microcracks occurring along the interface of sublayers were observed. Microstructural investigations of sprayed coatings showed the presence of randomly placed voids with an average size of 1.4 µm (Fig. 10d). The obtained coatings were built of particles with irregular shapes. Most of them had longitudinal shapes, which corresponds to the formation mechanism of plasma sprayed layers (Fig. 10b).

4. Discussion

Atmospheric plasma spraying (APS) performed with the help of given process parameters allow obtaining relatively thick (from ~ 100 up to ~ 300 µm) and dense coatings with low porosity. Thermal spraying techniques are widely applied to produce protective coatings, which are characterized by high hardness and wear resistance. Obtained coatings might improve functional properties and increase the durability of coated elements. Therefore, they are dedicated to the aerospace industry in order to surface protection of jet engine components [30], such as aero-engine cases as well as compressor blades and vanes.

The obtained investigation results showed that process parameters like powder feed rate, power current, and H_2/Ar gases flow ratio have a significant influence on coating microstructure, its thickness, and defects formation such as cracks and porosity.

Microstructure observations of carbide coatings proved that an increase in powder feed rate from 5 up to $20\,\mathrm{g\,min^{-1}}$ led to producing even four times thicker coating (~ 60 and ~ 260 µm) with slightly higher porosity of 7 and 9 %, respectively. The studies showed that the intermediate value of powder feed rate ($10\,\mathrm{g\,min^{-1}}$) allows for obtaining a relatively good ratio of coating thickness to porosity. The literature data indicate that the thickness of WC-Cr-Ni carbide coatings formed on the substrate of C15 unalloyed steel with the use of the APS method and similar process parameters were approximately 30 % thinner compared to our coatings described in the presented paper [29]. It could be due to the fact that coatings obtained by Kubaszek et al. were plasma sprayed with the use of lower values of power current.

The obtained findings showed that power current and H_2/Ar gases flow ratio affect both coating dense and also the formation of longitudinal cracks. Microstructure observations revealed that the application of only argon as plasma gas results in the formation of a coating with high porosity (14 %), which leads to a decrease in hardness and wear resistance. Moreover, an increase in the amount of hydrogen in the mixture of plasma gas up to 10 NLPM allowed for a reduction in the number of pores in the sprayed coating to 8 %. Plasma plume energy is dependent on power current and H_2/Ar gases ratio. The lower values of both parameters cause incomplete melting of the nickel matrix, which contributes to the brittle fracture of the coating. On the other hand, an increase in both parameters can affect the decomposition of carbide compounds, which has a significant effect on the hardness of sprayed coatings [31]. Based on ref. [32], the decomposition of carbides reduces also the wear resistance of coatings. Therefore, the appropriate selection of both parameters allows for obtaining the coating with the best properties.

The studies of the effect of power current on microstructure and porosity of coating revealed that its increase led to producing relatively thinner and porous coating (~ 180 µm for 350 A, ~ 120 µm for 550 A). Nevertheless, such torch currents could affect the decomposition of carbide, which contributes to the lowering of the mechanical properties of the coating. The results of our paper are comparable to those published by Bonache et al. [33]. They studied the effect of plasma on microstructure and wear properties of carbide WC-Co coating formed with the APS technique. It was found that plasma energy affects the tribological properties of the coating; hence lower values of torch power current provide growth of layer erosion resistance.

The carbide coatings obtained with the use of plasma spraying were built of characteristic longitudinal grains formed during the hit of molten particles on the coated substrate. Between them, local cracks propagating from equiaxed voids were observed. Moreover, the structure of WC-CrC-Ni coating consisted of randomly placed fine crystalline grains. A similar microstructure of carbide coatings produced on various substrates using APS and HVOF methods was observed in the previous works [31–34]. Unfortunately, the developed coatings, despite used spraying parameters, were characterized by higher porosity in comparison with HVOF-sprayed [3, 31–37].

The phase composition analysis based on received X-ray diffractograms helped to establish that APS carbide coatings were composed of the following phases WC, W_2C, Cr_3C_2, Cr_2O_3, and Cr_3Ni_2. The spectrum registered from the substrate material confirmed the presence of characteristic peaks corresponding to the hexagonal α-Ti phase, while for the coated sample, they completely disappeared. It is related to the considerable thickness of the layer in relation to the penetration depth of X-rays. The phase composition of WC-CrC-Ni coating is consistent with the results described by Fang et al. [3], who studied the same type of coating formed on IN718 nickel superalloy. In our further research, the erosion [36] and wear [37] resistance should be investigated.

5. Conclusions

The performed OM/SEM microstructure investigations allowed us to draw the following conclusions:

1. Increase of powder feed rate provides the increase of thickness of plasma sprayed WC-CrC-Ni carbide coating.

2. APS process performed at a flow rate of plasma gases H_2/Ar – 5/68, power current of 450 A, and 10 g min^{-1} of powder feed rate allows to obtain relatively thick (~ 140 μm) carbide coating with the lowest porosity (4 %).

3. Increase in the energy of the plasma plume could cause the decomposition of tungsten and chromium carbides, which are responsible for the hardness and wear resistance of coatings.

4. Plasma spraying at a lower torch power current allows producing the continuous coating with the lowest porosity.

5. Low hydrogen content in a mixture of plasma gases affects incomplete melting of the metallic matrix of coating material, which results in the formation of a more porous layer with low crack resistance.

References

[1] Ş. Danışman, D. Odabas, M. Teber, The effect of coatings on the wear behavior of Ti6Al4V alloy used in biomedical applications, IOP Conf. Ser.: Mater. Sci. Eng. 295 (2018) 012044. https://doi.org/10.1088/1757-899X/295/1/012044

[2] J. Mehta, V. K. Mittal, P. Gupta, Role of thermal spray coatings on wear, erosion and corrosion behavior: A review, Journal of Applied Science and Engineering 20 (2017) 445–452. https://doi.org/10.6180/jase.2017.20.4.05

[3] K. Szymański, A. Hernas, G. Moskal, H. Myalska, Thermally sprayed coatings resistant to erosion and corrosion for power plant boilers – A review, Surface and Coatings Technology 268 (2015) 153–164. https://doi.org/10.1016/j.surfcoat.2014.10.046

[4] M. R. Dorfman, Handbook of Environmental Degradation of Materials, 2005, Elsevier, pp. 405–422, ISBN: 9780815517498. https://doi.org/10.1016/B978-081551500-5.50022-7

[5] K. Murugan, A. Ragupathy, V. Balasubramanian, K. Sridhar, Optimizing HVOF spray process parameters to attain minimum porosity and maximum hardness in WC-10Co-4Cr coatings, Surface and Coatings Technology 247 (2014) 90–102. http://dx.doi.org/10.1016/j.surfcoat.2014.03.022

[6] J. Vicenzi, D. L. Villanova, M. D. Lima, A. S. Takimi, C. M. Marques, C. P. Bergmann, HVOF-coatings against high temperature erosion (300 °C) by coal fly ash in thermoelectric power plant, Materials and Design 27 (2006) 236–242. https://doi.org/10.1016/j.matdes.2004.10.008

[7] J. A. Picas, A. Forn, G. Matthäus, HVOF coatings as an alternative to hard chrome for pistons and valves, Wear 261 (2006) 477–484. https://doi.org/10.1016/j.wear.2005.12.005

[8] P. S. Babua„ P. Ch. Rao, A. Jyothirmayi, P. S. Phania, L. R. Krishnaa, D. S. Raoa, Evaluation of microstructure, property and performance of detonation sprayed WC-(W,Cr)2C-Ni coatings, Surface and Coatings Technology 335 (2018) 345–354. https://doi.org/10.1016/j.surfcoat.2017.12.055

[9] J. A. Picas, S. Menargues, E. Martin, C. Colominas, M. T. Baile, Characterization of duplex coating system (HVOF + PVD) on light alloy substrates, Surface and Coatings Technology 318 (2017) 326–331. http://dx.doi.org/10.1016/j.surfcoat.2016.06.020

[10] G. Bolelli, L.-M. Berger, M. Bonetti, L. Lusvarghi, Comparative study of the dry sliding wear behaviour of HVOF-sprayed WC-(W,Cr)$_2$C-Ni and WC-CoCr hardmetal coatings, Wear 309 (2014) 96–111. http://dx.doi.org/10.1016/j.wear.2013.11.001

[11] Š. Houdková, M. Kašparová, Experimental study of indentation fracture toughness in HVOF sprayed hardmetal coatings, Engineering Fracture Mechanics 110 (2013) 468–476. http://doi.org/10.1016/j.engfracmech.2013.05.001

[12] A. Rahbar-Kelishami, A. Abdollah-Zadeh, M. M. Hadavi, A. Banerji, A. Alpas, A. P. Gerlich, Effects of friction stir processing on wear properties of WC-12%Co sprayed on 52100 steel, Materials and Design 86 (2015) 98–104. http://dx.doi.org/10.1016/j.matdes.2015.06.132

[13] R. K. Kumar, M. Kamaraj, S. Seetharamu, S. Anan, S. Kumar, A pragmatic approach and quantitative assessment of silt erosion characteristics of HVOF and HVAF processed WC-CoCr coatings and 16Cr5Ni steel for hydro turbine applications, Materials and Design 132 (2017) 79–95. http://dx.doi.org/10.1016/j.matdes.2017.06.046

[14] B. C. Navinesh, B. Somasundaram, Jagadeeswaran, M. P. Mamatha, Better wear resistance of HVOF coating CrC-NiCrFeSiBCoC(35%–65%) and CrC-NiCrFeSiBCoC(80%–20%) on SS316 steels, Materials Today: Proceedings 20 (2020) 155–160. https://doi.org/10.1016/j.matpr.2019.10.094

[15] V. A. D. Souza, A. Neville, Linking electrochemical corrosion behaviour and corrosion mechanisms of thermal spray cermet coatings (WC/CrNi and WC/CrC-CoCr), Materials Science and Engineering 352 (2003) 202–211. https://doi.org/10.1016/S0921-5093(02)00888-2

[16] J. E. Cho, S. Y. Hwang, K. Y. Kim, Corrosion behavior of thermal sprayed WC cermet coatings having various metallic binders in strong acidic environment, Surface and Coatings Technology 200 (2006) 2653–2662. http://doi.org/10.1016/j.surfcoat.2004.10.142

[17] L.-M. Berger, S. Saaro, T. Naumann, M. Kašparová, F. Zahálka, Influence of feedstock powder characteristics and spray processes on microstructure and properties of WC-(W,Cr)$_2$C-Ni hardmetal coatings, Surface and Coatings Technology 205 (2010) 1080–1087. https://doi.org/10.1016/j.surfcoat.2010.07.032

[18] N. L. Parthasarathi, M. Duraiselvam, U. Borah, Effect of plasma spraying parameter on wear resistance of NiCrBSiCFe plasma coatings on austenitic stainless steel at elevated temperatures at various loads, Materials and Design 36 (2012) 141–151. http://doi.org/10.1016/j.matdes.2011.10.051

[19] A. S. Praveen, J. Sarangan, S. Suresh, J. S. Subramanian, Erosion wear behaviour of plasma sprayed NiCrSiB/Al_2O_3 composite coating, Int. Journal of Refractory Metals and Hard Materials 52 (2015) 209–218. http://dx.doi.org/10.1016/j.ijrmhm.2015.06.005

[20] Z.-Q. Zhang, H.-D. Wang, B.-S. Xu, G.-S. Zhang, Investigation on influence of WC-Ni addition on rolling contact fatigue behaviour of plasma sprayed Ni-based alloy coating, Tribology International 90 (2015) 509–518. http://doi.org/10.1016/j.triboint.2015.05.021

[21] G. M. Balamurugan, M. Duraiselvam, V. Anandakrishnan, Comparison of high temperature wear behaviour of plasma sprayed WC-Co coated and hard chromium plated AISI 304 austenitic stainless steel, Materials and Design 35 (2012) 640–646. http://doi.org/10.1016/j.matdes.2011.10.012

[22] P. W. Leech, X. S. Li, N. Alam, Comparison of abrasive wear of a complex high alloy hardfacing deposit and WC-Ni based metal matrix composite, Wear 294–295 (2012) 380–386. http://doi.org/10.1016/j.wear.2012.07.015

[23] D. Dzhurinskiy, A. Babu, P. Pathak, A. Elkin, S. Dautov, P. Shornikov, Microstructure and wear properties of atmospheric plasma-sprayed Cr_3C_2-NiCr composite coatings, Surface and Coatings Technology 428 (2021) 127904. https://doi.org/10.1016/j.surfcoat.2021.127904

[24] T.-S. Huang, Microstructure and properties of thermal sprayed WC-CrC-Ni coatings, China Steel Technical Report no. 24 (2011) 28–32.

[25] A. C. Murariu, N. Pleşu, I. A. Perianu, M. Tară-Lungă-Mihali, Investigations on corrosion behaviour of WC-CrC-Ni coatings deposited by HVOF thermal spraying process, Int. J. Electrochem. Sci. 12 (2017) 1535–1549. https://doi.org/10.20964/2017.02.60

[26] M. Richert, I. Nejman, M. Poręba, J. Sieniawski, Ł. Kuczek, Effect of plasma gases on the structure and properties of WC-CrC-Ni coatings, Key Engineering Materials 641 (2015) 105–110. https://doi.org/10.4028/www.scientific.net/KEM.641.105

[27] E. Jonda, L. Łatka, Comparative analysis of mechanical properties of WC-based cermet coatings sprayed by HVOF on to AZ31 magnesium alloy substrates, Advances in Science and Technology Research Journal 15 (2021) 57–64. https://doi.org/10.12913/22998624/135979

[28] P. Sosnowy, M. Góral, S. Kotowski, G. Hanula, J. Gwizdała, J. Drzał, M. Kobylarz, P. Borowski, R. Gargała, The influence of temperature on erosion resistance of carbide coatings deposited by APS method, Solid State Phenomena 227 (2015) 251–254. https://doi.org/10.4028/www.scientific.net/ssp.227.251

[29] T. Kubaszek, M. Góral, R. Różański, Ł. Szczepański, Influence of plasma spraying conditions on the microstructure and properties of WC-Cr-Ni metaloceramic layers, Journal of Metallic Materials 71 (2019) 3–7. https://doi.org/10.32730/imz.2657-747.19.2.1

[30] T. N. Rhys-Jones, The use of thermally sprayed coatings for compressor and turbine applications in aero engines, Surface and Coatings Technology 42 (1990) 1–11. https://doi.org/10.1016/0257-8972(90)90109-P

[31] V. Bolleddu, V. Racherla, P. P. Bandyopadhyay, Comparative study of air plasma sprayed and high velocity oxy-fuel sprayed nanostructured WC-17wt.%Co coatings, The International Journal of Advanced Manufacturing Technology 84 (2016) 1601–1613. https://doi.org/10.1007/s00170-015-7824-5

[32] J. Subrahmanyam, M. P. Srivastava, R. Sivakumar, Characterization of plasma-sprayed WC-Co coatings, Materials Science and Engineering 84 (1986) 209–214. https://doi.org/10.1016/0025-5416(86)90240-5

[33] V. Bonache, M. D. Salvador, J. C. García, E. Sánchez, E. Bannier, Influence of plasma intensity on wear and erosion resistance of conventional and nanometric WC-Co coatings deposited by APS, Journal of Thermal Spray Technology 20 (2011) 549–559. https://doi.org/10.1007/s11666-010-9572-2

[34] B. Venkateshwarlu, M. T. Basha B, A. Srikanth, Influence of critical carbide-cobalt plasma spray parameter coatings on microstructural and tribological characteristics of nanostructured tungsten carbide-cobalt coatings, Procedia Manufacturing 30 (2019) 339–346. https://doi.org/10.1016/j.promfg.2019.02.048

[35] W. Fang, T. Y. Cho, J. H. Yoon, K. O. Song, S. K. Hur, S. J. Youn, H. G. Chun, Processing optimization, surface properties and wear behavior of HVOF spraying WC-CrC-Ni coating, Journal of Materials Processing Technology 209 (2009) 3561–3567. https://doi.org/10.1016/j.jmatprotec.2008.08.024

[36] E. Jonda, M. Szala, L. Łatka, M. Walczak, Investigations of cavitation erosion and wear resistance of cermet coatings manufactured by HVOF spraying, Applied Surface Science 608 (2023) 155071. https://doi.org/10.1016/j.apsusc.2022.155071

[37] S. M. Pandey, Q. Murtaza, R. S. Walia, Study of dry wear behaviour and morphological characteristic of 60%Mo-20%NiCr-10%CrC-10%Mo+Fe based alloy coating by atmospheric plasma spray technique, Advances in Materials and Processing Technologies 3 (2017) 393–406. https://doi.org/10.1080/2374068X.2017.1334997